Journal of Neuroscience Methods 196 (2011) 182–189

Contents lists available at ScienceDirect

Journal of Neuroscience Methods

journal homepage: www.elsevier.com/locate/jneumeth

On the estimation of the direction of information flow in networks of dynamical systems

Linda Sommerlade[a,b,c,*], Florian Amtage[d], Olga Lapp[a,b], Bernhard Hellwig[d], Carl Hermann Lücking[d], Jens Timmer[a,b,c,e], Björn Schelter[a,b,c]

[a] Department of Physics, University of Freiburg, Hermann-Herder-Str. 3, 79104 Freiburg, Germany
[b] FDM, Freiburg Center for Data Analysis and Modeling, University of Freiburg, Eckerstr. 1, 79104 Freiburg, Germany
[c] Bernstein Center for Computational Neuroscience, University of Freiburg, Hansastr. 9A, 79104 Freiburg, Germany
[d] Department of Neurology and Clinical Neurophysiology, University of Freiburg, Breisacherstr. 64, 79106 Freiburg, Germany
[e] Freiburg Institute for Advanced Studies, Alberstr. 19, 79104 Freiburg, Germany

ARTICLE INFO

Article history:
Received 19 July 2010
Received in revised form
13 December 2010
Accepted 15 December 2010

Keywords:
Essential tremor
Direction of information flow
Maximum coherence
Partial directed coherence

ABSTRACT

The inference of the interaction structure in networks of dynamical systems promises novel insights into the functioning or malfunctioning of systems in the neurosciences. This may improve the understanding of mechanisms underlying several diseases like tremor disorders and might eventually help to cure patients. Of particular interest is the estimation of the direction of information flow for which different methods have been suggested and have been applied to data from human tremor. Based on a simulated system motivated by the human tremor application we analyze the performance of three methods. The abilities and limitations of the individual techniques are compared and discussed. An application to essential tremor complements this investigation.

1. Introduction

The analysis of signals in the neurosciences raises several questions. Of particular importance is the detection of interactions between signals, as they promise to disclose the biological basis underlying the normal behavior or the malfunctioning of certain networks (Grosse et al., 2002; Hellwig et al., 2000, 2001, 2003; Hesse et al., 2003; Tass et al., 1998; Volkmann et al., 1996). Several techniques to infer the interaction structure in complex networks have been proposed (e.g., Dahlhaus et al., 1997; Eichler et al., 2003; Rosenblum and Pikovsky, 2001; Smirnov and Bezruchko, 2003; Timmer et al., 1998a). Additionally, an inference towards the direction of information flow enables deeper insights into the underlying processes (Müller et al., 2003).

Two main approaches are followed to infer the direction of information flow. Firstly, several approaches exist that directly estimate the direction of information flow. These are methods based on, for instance, spectral analysis like the slope of the phase spectrum either preprocessed by subtracting the minimum phase information or not (Müller et al., 2003). Alternatively, several concepts have been suggested directly applying the concept of Granger-causality (Granger, 1969), like the Granger-causality index (Hesse et al., 2003), Geweke's measure for Granger causality (Geweke, 1982, 1984; Chen et al., 2006; Dhamala et al., 2008), the partial directed coherence (Baccalá and Sameshima, 2001; Sameshima and Baccalá, 1999), the directed partial correlation (Eichler, 2006) or the directed transfer function (Kamiński and Blinowska, 1991) with several modifications thereof, although the latter strictly speaking does not resemble Granger-causality (Eichler, 2006). Secondly, concepts that aim at inferring time lags between signals can also be utilized to estimate the direction of information flow by investigating the algebraic sign or signs of the estimated lags. These techniques include the maximum coherence (Govindan et al., 2005) approach in the framework of spectral analysis and methods based on the analytic amplitude or analytic phase of the signal (Timmermann et al., 2003).

We restrict ourselves here to a comparison of the performance in detecting the direction of information flow. This restriction is necessary as without such a restriction a meaningful comparison, on the one hand, would not be possible, and, on the other hand, it should not be considered a drawback per se that a technique does not provide the time lag between processes. As it finally turns out, the investigated methods that aim at inferring the direction based on the time lag of interaction perform actually

* Corresponding author at: FDM, Freiburg Center for Data Analysis and Modeling, University of Freiburg, Eckerstr. 1, 79104 Freiburg, Germany. Tel.: +49 761 203 7709; fax: +49 761 203 7700.
E-mail address: linda.sommerlade@fdm.uni-freiburg.de (L. Sommerlade).

0165-0270/$ – see front matter © 2011 Elsevier B.V. All rights reserved.
doi:10.1016/j.jneumeth.2010.12.019

worse than the analyzed technique just aiming at detecting the direction.

To compare different techniques we have chosen one representative of the different classes that was actually used already in tremor research. From the group of Granger causality measures the partial directed coherence was chosen because additionally to its prior application to tremor data it turned out that it performed well for the systems under investigation in a comparison study of Granger causality measures (Winterhalder et al., 2005). From the second class, we picked the maximum coherence approach as it was claimed to be more reliable in estimating the direction of information flow than the phase spectrum estimate and we picked the analytical signal based method of Timmermann et al. (2003) as a representative of this wide class of analysis techniques. We like to point out, that other promising methods for the detection of the direction of information flow exist. Thus, our conclusions will be restricted to the methods under investigation here.

The paper is organized as follows. In Section 2 we briefly introduce partial directed coherence, the fundamentals of cross-spectral analysis, the maximum coherence approach as well as the method estimating delay times based on analytical signals. Section 3 deals with a simulation study comparing the performance of the maximum coherence approach, the method based on analytical signal and partial directed coherence. We demonstrate the abilities and limitations also in an application to measured data originating from human tremor in Section 4.

2. Mathematical background

In this section the mathematical basis of the four techniques is briefly summarized.

2.1. Partial directed coherence

Vector autoregressive processes of order p (VAR[p]-process)

$$\begin{pmatrix} X_1(t) \\ \vdots \\ X_n(t) \end{pmatrix} = \sum_{u=1}^{p} \mathbf{a}(u) \begin{pmatrix} X_1(t-u) \\ \vdots \\ X_n(t-u) \end{pmatrix} + \begin{pmatrix} \varepsilon_1(t) \\ \vdots \\ \varepsilon_n(t) \end{pmatrix}, \tag{1}$$

in which the n processes under consideration are represented by an n-dimensional vector valued process $\mathbf{X}(t)$, are often utilized to model multivariate data. The coefficient matrices $\mathbf{a}_{kl}(u)$ ($k, l = 1, \ldots, n$; $u = 1, \ldots, p$) quantify the influence of process l on process k at a time lag u in the time domain.

The partial directed coherence $|\pi_{i\leftarrow j}(\omega)|$ for an n-dimensional (VAR[p]-process in the frequency domain is defined as (Baccalá and Sameshima, 2001).

$$|\pi_{i\leftarrow j}(\omega)| = \frac{\left|\mathbf{A}_{ij}(\omega)\right|}{\sqrt{\sum_m |\mathbf{A}_{mj}(\omega)|^2}} \tag{2}$$

with

$$\mathbf{A}(\omega) = I - \sum_{u=1}^{p} \mathbf{a}(u) \mathrm{e}^{-i\omega u}. \tag{3}$$

Again, the $\mathbf{a}(u)$ are the $n \times n$ coefficient matrices of the vector autoregressive model of order p.

Partial directed coherence $|\pi_{i\leftarrow j}(\omega)|$ provides a measure for the directed linear influence of $X_j(t)$ on $X_i(t)$ at frequency ω. It is estimated for realizations $x_i(t)$ and $x_j(t)$ of $X_i(t)$ and $X_j(t)$, respectively, by fitting an n-dimensional VAR[p]-model to the data and using Eqs. (2) and (3) with the parameter estimates $\hat{\mathbf{a}}_{ij}(u)$ substituting the true coefficients $\mathbf{a}_{ij}(u)$. A pointwise α-significance level for partial directed coherence $|\pi_{i\leftarrow j}(\omega)|$ is available (Schelter et al., 2005). This parametric approach is feasible to provide information about the direction of information flow based on a direct estimation and does not rely on time lag estimation first (e.g., Baccalá and Sameshima, 2001; Granger, 1969; Sameshima and Baccalá, 1999). Throughout the simulation studies in this paper we used $p = 21$. A nonzero entry in the covariance matrix of the noise term also correlates processes. Thus, two processes can be correlated even if there is no direct, causal connection. Since this influence is instantaneous in time, this correlation should be referred to as instantaneous interaction (Eichler, 2006; Mader et al., 2008), sometimes misleadingly also called instantaneous causality. Note that without investigating the covariance matrix instantaneous interactions cannot be dealt with.

2.2. Cross-spectral analysis

The maximum coherence approach is based on cross-spectral analysis which is briefly summarized here. The relationship between two stationary processes X_i and X_j can be investigated using cross-spectral analysis. For realizations $x_i(t)$ and $x_j(t)$ of length T the cross-correlation function estimate

$$\widehat{\mathrm{CCF}}_{x_i x_j}(\tau) = \langle x_i(t+\tau) x_j(t) \rangle_t \tag{4}$$

and the cross-spectrum estimate, which is the Fourier-transform of the $\widehat{\mathrm{CCF}(\tau)}$

$$\widehat{\mathrm{CS}}_{x_i x_j}(\omega) = \frac{1}{\pi} \int \widehat{\mathrm{CCF}}_{x_i y_j}(\tau) \mathrm{e}^{i\omega\tau} \mathrm{d}\tau, \tag{5}$$

are used. The linear interaction between the processes can be measured using the coherence which is the normalized modulus of the cross-spectrum

$$\widehat{\mathrm{Coh}}_{x_i x_j}(\omega) = \frac{\left|\widehat{\mathrm{CS}}_{x_i x_j}(\omega)\right|}{\sqrt{\widehat{S}_{x_i}(\omega)\widehat{S}_{x_j}(\omega)}} \quad \in [0, 1]$$

and by the phase spectrum

$$\hat{\Phi}_{x_i x_j}(\omega) = \arctan \frac{Im\widehat{\mathrm{CS}}_{x_i x_j}(\omega)}{Re\widehat{\mathrm{CS}}_{x_i x_j}(\omega)}$$

where $\hat{S}_{x_i}(\omega) = \widehat{\mathrm{CS}}_{x_i x_j}(\omega)$ for $i = j$ are the estimated auto-spectra of $x_i(t)$ and $x_j(t)$ and $\mathrm{Im}(\cdot)$ denotes the imaginary part while $\mathrm{Re}(\cdot)$ the real part of the complex valued cross-spectrum $\widehat{\mathrm{CS}}_{x_i x_j}(\omega)$.

The auto- and cross-spectra are estimated by dividing the time series of length N in l non-overlapping segments of length m. Each segment is tapered, then auto- and cross-periodograms are calculated and averaged over segments as suggested by (Bloomfield, 1976). Alternatively the auto- and cross-periodograms can be calculated for the whole time series and smoothed afterwards to get a consistent estimate for the auto- and cross-spectra (Priestley, 1989).

The variance of the coherence

$$var[\widehat{\mathrm{Coh}}_{x_i x_j}(\omega)] = \frac{1}{\nu}(1 - |\mathrm{Coh}_{x_i x_j}(\omega)|^2), \tag{6}$$

where ν denotes the number of degrees of freedom, which depends on the number of segments and the taper window (Bloomfield, 1976), is functionally releated to the true coherence and is therefore not directly accessible. An estimator is given by substituting the estimated coherence in Eq. (6). Under the null hypothesis of zero coherence a critical value for significance level α is given by

$$s = \sqrt{1 - (1-\alpha)^{1/((\nu/2)-1)}}.$$

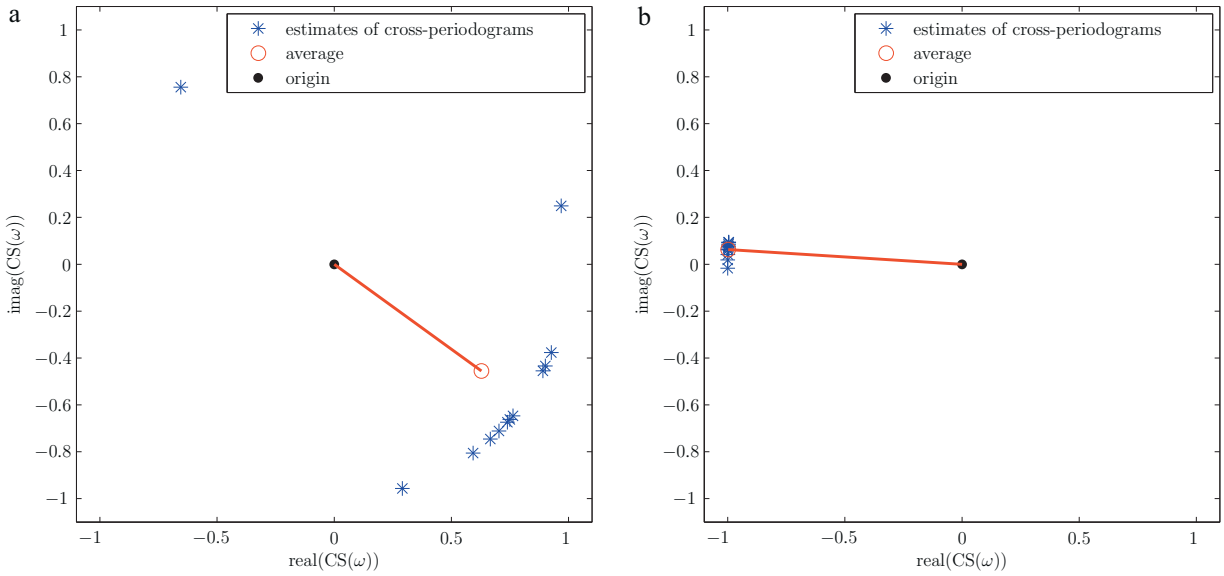

Fig. 1. Values of the cross-periodograms at one single frequency estimated from a simulated AR[2]-process and its delayed copy are displayed as asterisks. The mean is denoted with a circle. (a) The delay between the copies was set to 100 sampling points. (b) The delay between the copies was set to 10 sampling points. In (b) the misalignment effect is hardly visible, therefore the mean is displayed in red color. (For interpretation of the references to color in this figure legend, the reader is referred to the web version of the article.)

2.2.1. Estimation using the maximum coherence approach

To estimate the direction of information flow, the maximum coherence approach uses the so-called misalignment effect, which occurs in cross-spectral analysis. Misalignment is caused by a locally changing phase spectrum, as for instance present for a delay between the considered time series. It manifests itself in a spurious reduction of the estimated coherence (Hannan and Thomson, 1971). This reduction arises in the estimation procedure for instance when the data segments are averaged. Fig. 1 illustrates this scenario: We analyzed a realization of an AR[2] process and its delayed copy. The normalized values of the cross-periodograms of the datasets for one single frequency are displayed (Fig. 1(a)). Due to the large variance of the phase of the estimated cross-periodograms the values are blurred over a large segment of the unit circle. The average of these values falls inside the unit circle and, thus, its absolute value is below the true coherence value of 1, which we would obtain if there was no time delay between the time series. Fig. 1(b) shows the effect for a smaller delay.

The main idea of the maximum coherence approach is to introduce artificial time lags between the time series to compensate for the true time delay between the time series, until the coherence takes its maximum. Thus, the coherence $\widehat{\mathrm{Coh}}(\tau)$ is considered as a function of the time lag τ evaluated at a certain frequency ω_{ref}. This leads to the estimator

$$\hat{\tau} = arg\max_{\tau} \widehat{\mathrm{Coh}}(\tau)$$

for the delay between processes X_i and X_j. If the maximum occurs for positive delays, process $X_i(t)$ influences $X_j(t)$, while this is the opposite if the maximum is found for negative delays. Note that the same arguments and ideas also hold when estimating the spectra based on smoothing the periodograms.

The maximum coherence method was claimed to be superior to methods utilizing the phase spectrum because it is still applicable even if high coherence values are limited to a narrow frequency band (Govindan et al., 2005).

2.3. Estimation based on the analytic signal

For estimating the direction of information flow based on the analytic signal as suggested by (Timmermann et al., 2003), both signals are required to be narrow band pass filtered around the oscillation frequency of the signal showing a distinct oscillation. We follow here the procedure of Timmermann et al. (2003) by setting the bandwidth to ±2 Hz. The Hilbert transform is applied to both filtered real-valued signals x_i and x_j leading to the so-called analytic signal

$$z_j(t) = x_j(t) + i\tilde{x}_j(t),$$

where the imaginary counterparts of x_i and x_j are obtained from the Hilbert transform. This allows a separation of phase and amplitude as

$$z_j(t) = x_j(t) + i\tilde{x}_j(t) = A_j(t)e^{i\Phi_j(t)}.$$

The amplitudes of x_i and x_j are denoted by $A_i(t)$ and $A_j(t)$, whereby the phases are denoted by $\Phi_i(t)$ and $\Phi_j(t)$, respectively.

Following Timmermann et al. (2003), from the Hilbert amplitude of the signal showing a distinct oscillation, the times of maximum amplitudes are detected. The instantaneous phase differences between both signals at these times of maximum amplitude are computed. Phase differences between the two signals are then transferred into directions of information flow based on the phase differences. A positive phase difference indicates that process $x_i(t)$ influences $x_j(t)$ and vice versa for negative phase differences. The maximum of the histogram of these phase differences is used to collapse the whole set of phase differences in one single direction of information flow.

3. Application to simulated data

To compare the performances of partial directed coherence, the maximum coherence approach, and the method based on the analytic signal, we applied them to simulated data. The simulated systems are motivated by the intention to apply the methods to data from human tremor.

Before we discuss the simulations, we mention that for the methods based on phases, one always obtains both directions of information flow just due to the fact that the phase is 2π periodic. Since this 2π periodicity does not reflect actual delays present in the data, we have decided to focus only on those directions of information flow that are associated with delays present in the data. This can be achieved in our simulations as we know the true directions and delays.

3.1. Sensory feedback

Here, the motor cortex is assumed to generate the tremor, thus we assumed a generator $x(t)$ and its projection to the tremorous muscle $y(t)$. The feedback of the muscle in this simulation is only received by the sensory part of the cortex and therefore it enters only the observation and not the dynamics of $x(t)$. Thus, assuming that simultaneously to the motor also the sensory part of the cortex is measured, $y(t)$ enters the observation of $x(t)$. We consider this a naive model for human tremor as in this simplified model the brain does not process the feedback from the muscles. Nevertheless, an analysis technique aiming at the estimation of the direction of information flow should be able to handle this scenario.

For the generator $x(t)$ we choose an autoregressive process of order two (AR[2]). The projection $y(t)$ is modeled as a time shifted copy of it

$$x(t) = a_1 x(t-1) + a_2 x(t-2) + \varepsilon_x(t), \tag{7}$$

$$y(t) = c \times x(t-\Delta) + \varepsilon_y(t). \tag{8}$$

We used standard Gaussian noise $\varepsilon_{x,y} \in N(0, \sigma^2_{x,y})$, $\sigma^2_{x,y} = 1$, $c = 1$, $a_1 = 0.32$ and $a_2 = -0.036$. Assuming a sampling rate of 1000 Hz this corresponds to a driven damped oscillator with characteristic frequency $\omega_0 = 5$ Hz and relaxation time $\tau = 600$ ms. We assume that $y(t)$ enters the observation of $x(t)$ as proprioceptive feedback with the same delay $\Delta = 20$ ms, thus

$$x_{\mathrm{obs}}(t) = x(t) + d \times y(t-\Delta) \tag{9}$$

and

$$y_{\mathrm{obs}} = y(t) \tag{10}$$

are observed. We choose d between 0 and 1 in steps of 0.1. The simulated time series had a length of 40 s, with the assumed sampling rate of 1000 Hz this corresponds to 40,000 data points. For each parameter d, 100 realizations were simulated.

For $d = 0$, the system represents a pure signal propagation, where $y(t)$ is a delayed copy of $x(t)$. As actual signals are not expected to be completely identical, we added white noise process to $y(t)$. All techniques are capable of correctly revealing the direction of information flow in this case. The results for the maximum coherence are shown in Fig. 2, those for the analytical signal based technique are depicted in Fig. 3. For the partial directed coherence the results are shown in Fig. 4. By choosing parameter d to be non-zero, in the model $x_{\mathrm{obs}}(t)$ contains two terms, one of which is the influencing dynamics, while the other presents a delayed feedback of $y(t)$ onto $x(t)$. This delayed feedback, however, does not alter the dynamics present in $x(t)$. The parameter d quantifies the strength of the feedback. All techniques but the partial directed coherence detect only the dominant direction of information flow, which is for all parameters from $d = 0$ to $d = 1$ the one from $x(t)$ onto $y(t)$. Only partial directed coherence is correctly estimating the present directions of information flow in all cases, i.e., irrespective of whether there is feedback or not (Figs. 4 and 5).

The maximum coherence approach was claimed to detect both directions of interaction (Raethjen et al., 2007) if two maxima are present, one for a positive delay and one for a negative delay. In our simulation, we could not reproduce this result other than in scenarios, in which the fluctuations of the estimated coherence values are rather high. This can be achieved only for small values of the number of degrees of freedom (cf. Eq. (6)). To substantiate this, we show in Fig. 6 the influence of the block length used to estimate coherence on the estimation of the time lag, which is used to estimate the direction of information flow. As a model system we used here the illustrative example of an AR[2] process (Eq. (7)) and its driving noise $\varepsilon(t)$ shifted by 400 timesteps. The oscillation frequency of the AR[2] process was varied between 4 and 5 Hz in steps of 0.1 Hz to investigate the dependence on the block length for various frequencies. The range between 4 and 5 Hz is again typically found in pathological tremor. Different lengths of the segments were used for averaging the periodograms. The segment-length was set to 0.5, 1, 2, 4 and 8 s, respectively. Additionally, a spectral estimator based on smoothing the periodograms (Priestley, 1989) was used. For each scenario 10 realizations were simulated.

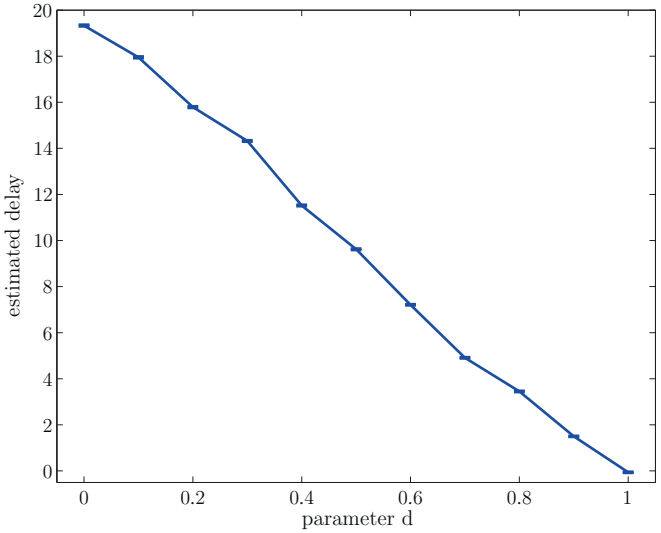

Fig. 2. Delay times and therefore direction of information flow estimated for the simulated data using the maximum coherence approach. For each parameter d the mean of the 100 realizations and its standard deviation are shown. Only the direction from the $x(t)$ onto $y(t)$ is detected.

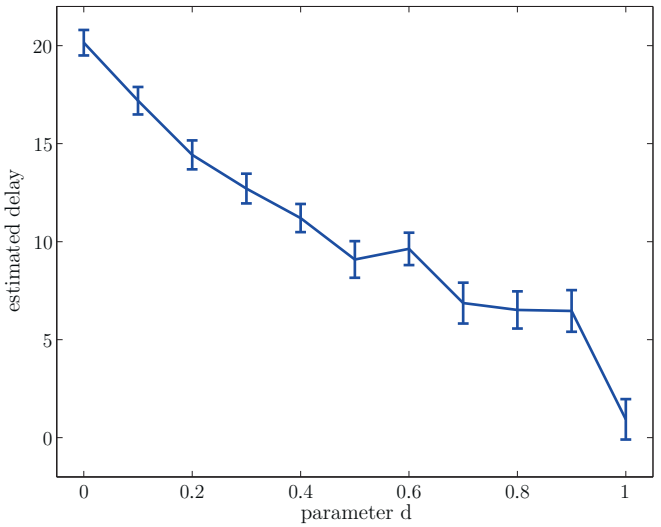

Fig. 3. Delay times and therefore direction of information flow estimated for the simulated data using the analytical signal based techniques. For each parameter d the mean of the 100 realizations and its standard deviation are shown. Only the direction from the $x(t)$ onto $y(t)$ is detected.

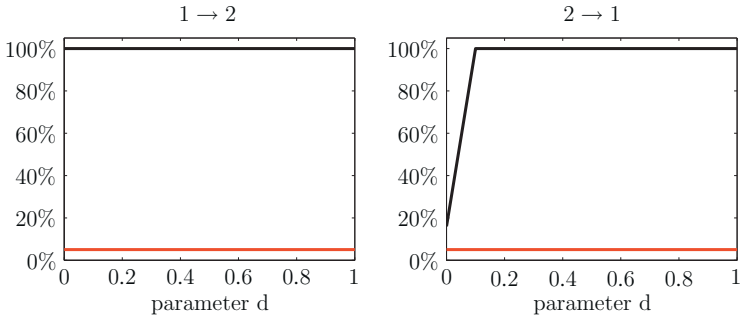

Fig. 4. Direction of information flow estimated for the simulated data using the partial directed coherence. For each parameter d the percentage of the 100 realizations with significant partial directed coherence are shown. A significance-level of 5% was used. The direction from process 1 onto 2 is detected for all values of d, while the opposite direction is only detected for the non-zero values of d.

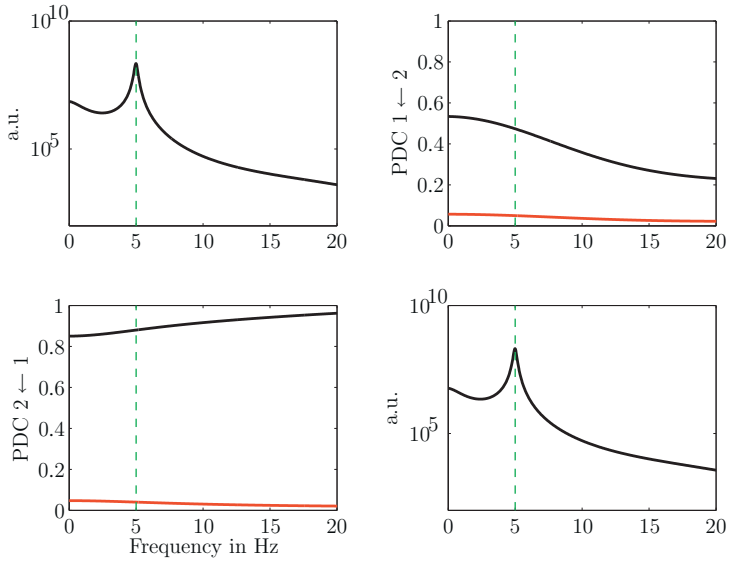

Fig. 5. Exemplary result of partial directed coherence analysis for one realization with $d = 0.1$ and model order $p = 21$. On the diagonal the auto-spectra of the two processes are depicted. Off-diagonal figures represent partial directed coherence. The 5%-significance level is depicted as a red line. Green dashed lines indicate the dominant frequency of the processes. (For interpretation of the references to color in this figure legend, the reader is referred to the web version of the article.)

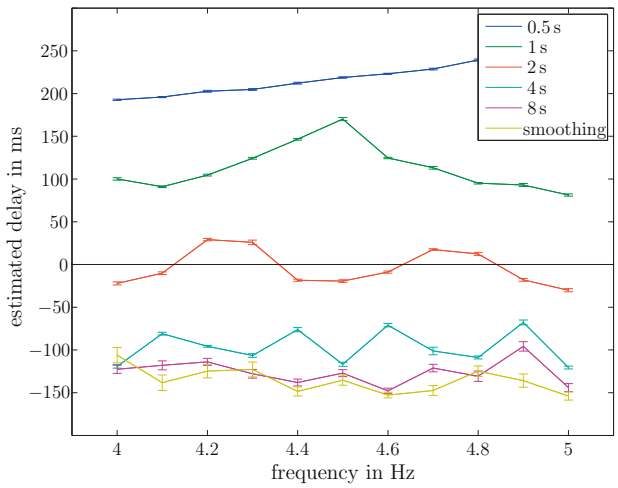

Fig. 6. Delay times estimated for the simulated data using the maximum coherence approach. Coherence was analyzed at the oscillation frequency of the AR[2] process. For each frequency and segment-length the mean of 10 realizations and its standard deviation are shown.

Fig. 6 demonstrates that the lag estimated using the maximum coherence approach depends on the length of the segments used. In critical cases for which the lag is close to zero this might lead to a change in the algebraic sign of the lag and therefore to a false positive detection of the direction of the information flow. Knowing that the phase relation between an AR[2] process and its driving noise has a steep negative slope at the oscillation frequency, the results can be understood as follows. The segment-length used for averaging the periodograms determines the frequency resolution of the spectra. Short segments lead to a rather rough sampling of the phase relation. Thereby, the steep slope cannot be resolved – it seems less steep. Since the maximum coherence approach corrects for the slope in the phase spectrum, the estimated lag increases with increasing resolution of the slope achieved by longer segments. This in turn is reflected in the estimates of the direction of information flow which is based on the lags.

Since in applications the "truth" is not known in advance, an estimator for the time lag and therefore eventually for the direction of information flow that depends on the chosen length of the segments is difficult to interpret. As obtained from the simulations, without a profound knowledge of the optimal length of the segments no reliable estimation of the direction of information flow is possible using the maximum coherence approach.

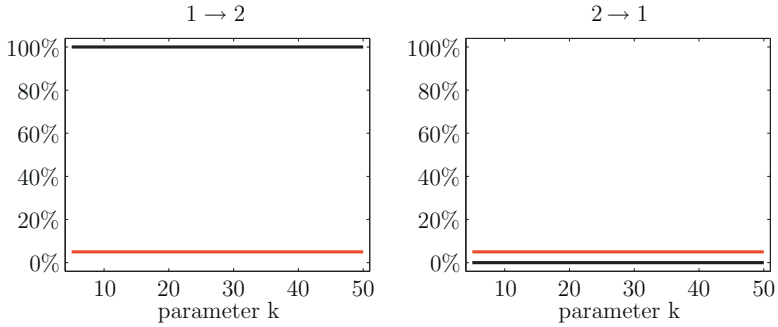

Fig. 7. Direction of information flow estimated using maximum coherence and the analytical signal based approach for the reflex model with $k = 5$ to $k = 50$ in steps of 5. For each parameter value the percentage of the 100 realizations detecting the specific direction are shown.

3.2. Dynamic feedback

In a second simulation scenario, the feedback of the muscle enters also the motor part of the cortex and therefore it enters the dynamics of $x(t)$. The model represents a reflex mechanism. As before, the motor cortex $x(t)$ is assumed to generate the tremor and modeled as an autoregressive process of order two (AR[2]). The projection to the muscle $y(t)$ is represented as a time shifted copy of it. The feedback is modeled according to (Timmer et al., 1998b)

$$x(t) = a_1 x(t-1) + a_2 x(t-2) + \varepsilon_x(t) + k \times \tanh(y(t - \Delta_{\text{feedback}})), \quad (11)$$

$$y(t) = c \times x(t - \Delta_{\text{projection}}) + \varepsilon_y(t). \quad (12)$$

We used standard $\varepsilon_{x,y} \in N(0, \sigma^2_{x,y})$, $\sigma^2_{x,y} = 1$, $c = 1$, $a_1 = 0.32$ and $a_2 = -0.036$. Assuming a sampling rate of 1000 Hz this corresponds to a driven damped oscillator with characteristic frequency $\omega_0 = 5$ Hz and relaxation time $\tau = 600$ ms. The delay $\Delta_{\text{projection}} = \Delta_{\text{feedback}} = 20$ ms was fixed, while we tested different values of the strength of the reflex k. The simulated time series had again a length of 40 s, with the assumed sampling rate of 1000 Hz this corresponds to 40,000 data points. As before, 100 realizations were simulated.

The maximum coherence approach, estimated again only one direction of information flow for all 100 realizations (Fig. 7). The feedback of $y(t)$ to $x(t)$ is not revealed by this analysis methods. Analogously the method based on the analytic signals only detects the influence of $x(t)$ onto $y(t)$. Using partial directed coherence, the connection from $x(t)$ onto $y(t)$ was revealed in 100% of the realizations for small $k = 5$ and in more than 85% of the cases for k smaller than 50, which corresponds to a reflex strength of 10% of the variance of $x(t)$ without the reflex. The feedback of $y(t)$ to $x(t)$ was also detected in more than 85% of the realizations for k smaller than 50 (Fig. 8).

Thus, again partial directed coherence is superior to maximum coherence and the method based on the analytical signal.

4. Application to essential tremor

Essential tremor is a common neurodegenerative disease which manifests itself mainly in the upper limbs, the tremor frequency of the hand is 4–8 Hz. To elucidate the tremor generating mechanisms in essential tremor, relationships between cortical and muscular activity are of particular interest. Cortical involvement in essential tremor has been found in various studies (Hellwig et al., 2001; Raethjen et al., 2007; Schnitzler et al., 2009). The question arises whether the cortex imposes its oscillatory activity on the muscles via the corticospinal tract or whether the muscle activity is just reflected in the cortex via proprioceptive afferences. No consistent results could be found by analyzing the phase spectra, as discussed in Hellwig et al. (2000, 2001).

Seven patients (four women, three men) with essential tremor participated in the study. All patients were selected because they showed a postural tremor of the arms without significant head tremor. Patients were on average 60.3 years of age (range 45–73 years). Tremor had been present for at least 5 years (mean 18.7 years; range 5–45 years). Apart from the postural tremor in the arms, there was no evidence of further neurological abnormalities, particularly Parkinsonian symptoms. All patients gave informed consent to participate in the study.

During the recordings, patients were seated in a comfortable chair inside a dimly lit room with their forearms supported. Surface EMG electrodes were attached to the wrist flexors and extensors of both arms. EEG recording was done with a 64-channel EEG system (Neuroscan, Herndon, VA, USA). Patients were asked to keep their eyes open and to fix their eyes on a point of light about 1.5 m away. Postural tremor was elicited by unilateral wrist extension on the right or the left side. To increase the tremor amplitude, some patients were instructed to count backwards mentally. EEG and EMG signals were sampled at 1000 Hz and band-pass filtered (EEG 1–200 Hz, EMG 50–200 Hz). The EMG was full-wave rectified.

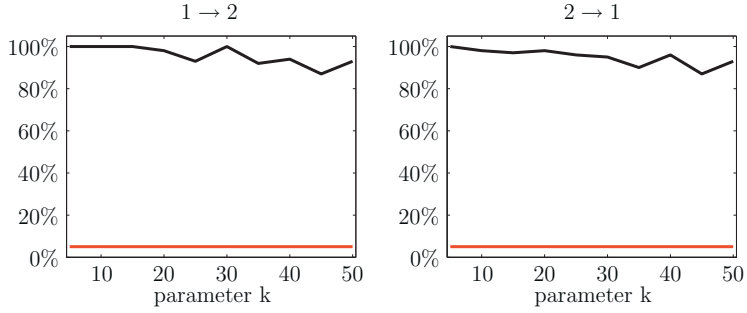

Fig. 8. Direction of information flow estimated using partial directed coherence for the reflex model with $k = 5$ to $k = 50$ in steps of 5. For each parameter value the percentage of the 100 realizations with significant partial directed coherence are shown. A significance-level of 5% was used.

Table 1
Directions estimated using maximum coherence, the method based on the analytical signal and partial directed coherence. For the maximum coherence approach two different segment-lengths were used. '–' indicates that no maximum was found in the range of ±300 ms. n.s. denotes that coherence was not significant at the tremor frequency. For the analytical signal based approach a spectral estimator based on smoothing periodograms with a smoothing width of 0.2 Hz was used. Partial directed coherence was check for significance at the tremor frequency using 5%-significance level and a model order of $p = 100$.

Patient	Trial	Maximum coherence		Analytical signal	PDC
		1 s segments EMG–EEG	2 s segments EMG–EEG	EMG–EEG	EMG–EEG
1	1	↔	→	→	→
1	2	→	→	←	↔
2	1	↔	←	→	↔
2	2	→	←	←	↔
3	1	→	n.s.	←	→
3	2	←	–	←	→
3	3	n.s.	n.s.	n.s.	→
4	1	→	→	→	→
4	2	→	n.s.	←	↔
4	3	→	→	←	↔
4	4	→	←	←	→
5	1	←	n.s.	←	→
5	2	n.s.	n.s.	n.s.	→
5	3	n.s.	n.s.	n.s.	←
6	1	–	n.s.	n.s.	→
6	2	–	–	→	→
7	1	→	n.s.	n.s.	↔
7	2	→	→	←	→
7	3	n.s.	←	←	↔
		EMG–EEG	EMG–EEG	EMG–EEG	EMG–EEG

For each patient a different number of trials was analyzed depending on the tremor activity. Whether tremor was dominant in the left and/or right side was determined by the auto-spectra of the EMG channels. A prominent peak in the range of 4–8 Hz was used as an indicator of dominant tremor.

To demonstrate that the results obtained in the simulation study are actually valid for the tremor study investigated here, the maximum coherence approach was applied to the data using two different segment-lengths, 1 and 2 s, respectively. The estimated directions for all methods are summarized in Table 1. The results for 1 and 2 s windows are not consistent with one another. Frequently, directions of information flow for the 1 s window are not present in the 2 s window analysis or in some cases even reversed. This unexpected behavior, which renders the results of techniques hardly interpretable, can be understood from the simulation studies and resembles the results found in Section 3.1.

Using the method based on the analytical signal, for each trial only the most prominent peak was evaluated disregarding secondary peaks due to the 2π periodicity. All trials were analyzed at the tremor frequency determined by the auto-spectra. As discussed in Section 3 the analytical signal based approach can only detect one direction of influence. We found an influence from EMG to EEG in four of the 19 trials. The opposite direction was found in ten of the trials. The ramaining five trails showed no significant coherence at the tremor frequency using a spectral estimator based on smoothing periodograms with a smoothing width of 0.2 Hz.

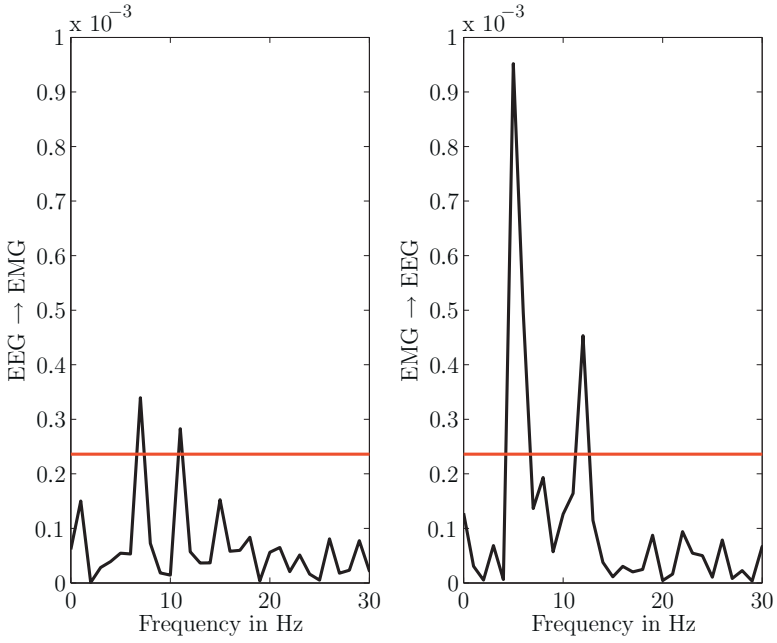

Fig. 9. Exemplary results of the partial directed coherence analysis for the left EMG and the right EEG channel of trial 3 of patient 4. A model order of $p = 100$ was used. The 5%-significance level is depicted in red. For both directions partial directed coherence exceeds the significance level at the tremor frequency of approximately 7 Hz. (For interpretation of the references to color in this figure legend, the reader is referred to the web version of the article.)

Partial directed coherence was estimated for EMG and the corresponding contra lateral EEG with model order $p = 100$. Data were down-sampled to a sampling rate of 100 Hz. A 5%-significance level was used. In Table 1 the results for all seven patients are summarized.

In Fig. 9, exemplary results of the partial directed coherence analysis of trial 3 of patient 4 are shown. Significant partial directed coherences at the tremor frequency are detected for the direction from the left EMG to the right, contra lateral EEG, and vice versa.

For both directions of interaction we tested for significant partial directed coherence at the tremor frequency. In 18 of the 19 analyzed trials a significant influence of EMG on the contra lateral EEG was found. In 9 trials we detected also the direction from EEG to EMG. In Fig. 9 the partial directed coherence indicating a causal influence from EMG to EEG is much higher than the partial directed coherence indicating a causal influence from EEG to EMG. This is a general observation that is also reflected in the number of trials in which we found a directed influence from the cortex to the muscles which is lower than the number of trials with a directed influence from the muscles to the cortex. As discussed in Schelter et al. (2005) this is due to the the different signal-to-noise-ratios of the individual signals.

In summary, since causal influences from the EEG to the corresponding contra lateral EMG are present, participation of the motor cortex in tremor generation is strongly indicated. Moreover, there is also a significant partial directed coherence from the EMG to the contra lateral EEG at the tremor frequency. This corresponds to a feedback from the muscles to the sensorimotor cortex.

5. Conclusion

We compared the maximum coherence, a method based on analytical signal, and partial directed coherence, as measures for the direction of information flow. Based on a simulation study motivated by an actual application, we demonstrated that if for two processes both directions of interaction are present the maximum coherence approach as well as the method based on analytical signals lead to erroneous results. From the methods investigated here, only partial directed coherence was able to detect all interactions present reliably. Moreover, we could show that the maximum coherence approach strongly depends on the estimation procedure, which we consider a severe problem in applications.

We presented an application to data measured from human tremor. Using partial directed coherence we found both directions of interaction in almost every second analyzed trial of the seven patients. This suggests a feedback loop from the cortex to the muscles via the corticospinal tract and from the muscles to the cortex via somatosensory afferences. The existence of this feedback loop indicates that the cortex is a recipient of proprioceptive input and contributes actively to the clinical expression of tremor.

In conclusion, several techniques exist to estimate the direction of information flow. Some of these even promise to infer the time lag between the influencing and influenced process. From the simulation studies presented here, one can infer that the specific techniques are not able to provide the actual direction of information flow. Thus, it is mandatory to perform a tailored simulation study before applying the techniques to actual signals. Such a performance test allows rigorous conclusions from the results of the analyses applied to measured data.

Acknowledgements

This work was supported by the German Science Foundation (Ti315/4-2), the German Federal Ministry of Education and Research (BMBF grant 01GQ0420), and the Excellence Initiative of the German Federal and State Governments. B.S. and L.S. are indebted to the Landesstiftung Baden-Württemberg for the financial support of this research project by the Eliteprogramme for Postdocs.

References

Baccalá LA, Sameshima K. Partial directed coherence: a new concept in neural structure determination. Biol Cybern 2001;84:463–74.
Bloomfield P. Fourier analysis of time series: an introduction. New York: John Wiley & Sons; 1976.
Chen Y, Bressler SL, Ding M. Frequency decomposition of conditional Granger causality and application to multivariate neural field potential data. J Neurosci Methods 2006;150:228–37.
Dahlhaus R, Eichler M, Sandkühler J. Identification of synaptic connections in neural ensembles by graphical models. J Neurosci Methods 1997;77:93–107.
Dhamala M, Rangarajan G, Ding M. Estimating Granger causality from Fourier and wavelet transforms of time series data. Phys Rev Lett 2008;100:018701.
Eichler M. Graphical modeling of dynamic relationships in multivariate time series. In: Schelter B, Winterhalder M, Timmer J, editors. Handbook of time series analysis. Wiley-VCH; 2006. p. 335–72 [chapter 14].
Eichler M, Dahlhaus R, Sandkühler J. Partial correlation analysis for the identification of synaptic connections. Biol Cybern 2003;89:289–302.
Geweke J. Measurement of linear dependence and feedback between multiple time series. J Am Stat Assoc 1982;77:304–13.
Geweke J. Measures of conditional linear dependence and feedback between time series. J Am Stat Assoc 1984;79:907–15.
Govindan RB, Raethjen J, Kopper F, Claussen JC, Deuschl G. Estimation of time delay by coherence analysis. Physica A 2005;350:277–95.
Granger J. Investigating causal relations by econometric models and cross-spectral methods. Econometrica 1969;37:424–38.
Grosse P, Cassidy MJ, Brown P. EEG-EMG and MEG-EMG and EMG-EMG frequency analysis: physiological principals and clinical applications. Clin Neurophysiol 2002;113:1523–31.
Hannan E, Thomson P. The estimation of coherency and group delay. Biometrika 1971;58:469–81.
Hellwig B, Häußler S, Lauk M, Köster B, Guschlbauer B, Kristeva-Feige R, et al. Tremor-correlated cortical activity detected by electroencephalography. Electroenceph Clin Neurophys 2000;111:806–9.
Hellwig B, Häußler S, Schelter B, Lauk M, Guschlbauer B, Timmer J, et al. Tremor correlated cortical activity in essential tremor. Lancet 2001;357:519–23.
Hellwig B, Schelter B, Guschlbauer B, Timmer J, Lücking C. Dynamic synchronisation of central oscillators in essential tremor. Clin Neurophysiol 2003;114:1462–7.
Hesse W, Möller E, Arnold M, Schack B. The use of time-variant EEG Granger causality for inspecting directed interdependencies of neural assemblies. J Neurosci Methods 2003;124:27–44.
Kamiński MJ, Blinowska KJ. A new method of the description of the information flow in the brain structures. Biol Cybern 1991;65:203–10.
Mader W, Feess D, Lange R, Saur D, Glauche V, Weiller C, et al. On the detection of direct directed information flow in fMRI. IEEE J Sel Top Signal Process 2008;2:965–74.
Müller T, Lauk M, Reinhardt M, Hetzel A, Lücking C, Timmer J. Estimation of time-delays in biological systems. Ann Biomed Eng 2003;31:1423–39.
Priestley MB. Spectral analysis and time series. London: Academic Press; 1989.
Raethjen J, Govindan RB, Kopper F, Muthuraman M, Deuschl G. Cortical involvement in the generation of essential tremor. J Neurophysiol 2007;97:3219–28.
Rosenblum MG, Pikovsky AS. Detecting direction of coupling in interacting oscillators. Phys Rev E 2001;64, 045202(R).
Sameshima K, Baccalá LA. Using partial directed coherence to describe neuronal ensemble interactions. J Neurosci Methods 1999;94:93–103.
Schelter B, Winterhalder M, Eichler M, Peifer M, Hellwig B, Guschlbauer B, et al. Testing for directed influences among neural signals using partial directed coherence. J Neurosci Methods 2005;152:210–9.
Schnitzler AC, Münks MB, Timmermann L, Gross J. Synchronized brain network associated with essential tremor as revealed by magnetoencephalography. Mov Disord 2009;24:1629–35.
Smirnov DA, Bezruchko BP. Estimation of interaction strength and direction from short and noisy time series. Phys Rev E 2003;68:046209.
Tass P, Rosenblum MG, Weule J, Kurths J, Pikovsky AS, Volkmann J, et al. Detection of n:m phase locking from noisy data: application to magnetoencephalography. Phys Rev Lett 1998;81:3291–5.
Timmer J, Lauk M, Pfleger W, Deuschl G. Cross-spectral analysis of physiological tremor and muscle activity. I. Theory and application to unsynchronized EMG. Biol Cybern 1998a;78:349–57.
Timmer J, Lauk M, Pfleger W, Deuschl G. Cross-spectral analysis of physiological tremor and muscle activity. II. Application to synchronized EMG. Biol Cybern 1998b;78:359–68.
Timmermann L, Gross J, Dirks M, Volkmann J, Freund H-J, Schnitzler A. The cerebral oscillatory network of Parkinsonian resting tremors. Brain 2003;126:199–212.
Volkmann J, Joliot M, Mogilner A, Ioannides AA, Lado F, Fazzini E, et al. Central motor loop oscillations in Parkinsonian resting tremor revealed by magnetoencephalography. Neurology 1996;46:1359–70.
Winterhalder M, Schelter B, Hesse W, Schwab K, Leistritz L, Klan D, et al. Comparison of linear signal processing techniques to infer directed interactions in multivariate neural systems. Signal Process 2005;85:2137–60.